PERGAMON

Vision Research 43 (2003) 1177–1185

Vision Research

www.elsevier.com/locate/visres

Neural fine tuning during Vernier acuity training?

Kristian Folta *

Westf. Wilhelms Universität, FB07, D-48149 Münster, Germany

Received 14 March 2002; received in revised form 2 December 2002

Abstract

A superposition masking and summation to threshold paradigm was employed before and after unmasked Vernier acuity training to measure sensory changes of offset analysing mechanisms.

Masking functions show a uniform downward translation after training and detection data reveal higher sensitivities to compound Gabor gratings in the post-test.

These findings confirm the existence of learning related changes at early levels of information processing, but the results cannot be explained by neural fine tuning of offset analysing mechanisms. The data are consistent with the idea of task dependent broadening of orientation tuned mechanisms responsible for detecting small Vernier offsets.

Keywords: Hyperacuity; Masking; Perceptual learning; Vernier acuity

1. Introduction

Human observers demonstrate an exquisite ability to judge whether a pair of target features is aligned or misaligned. This ability is known as Vernier acuity. Under optimal conditions, Vernier thresholds are considerably smaller than the eye's blur function or the foveal cone diameter (Westheimer, 1975). The fine precision with which Vernier tasks can be performed has long been of interest to vision scientists. One general hypothesis states the outputs of orientation and size tuned mechanisms as an important source of information by which the visual system may accomplish Vernier acuity. This notion is supported by findings that orientation masking of Vernier acuity with oblique grating or plaid masks produces bimodal peak threshold elevations at about 10°–20° on each side of Vernier target orientation (Carney & Klein, 1991; Findlay, 1973; Levi & Waugh, 1996; Mussap & Levi, 1995, 1996, 1997; Waugh, Levi, & Carney, 1993). Similar shapes of threshold elevation with plaid and grating masks suggest that Vernier offsets are detected on the basis of the pooled differential activity of orientation tuned mechanisms (i.e. absolute, rather than relative activity), with pooling occurring between mechanisms tuned to the same orientation but to adjacent positions relative to the axis of the target and between mechanisms of different orientation tuning in the same position. This model, known as the line-element model, is a general model applied to Vernier tasks as well as to other hyperacuity tasks (Wilson & Gelb, 1984; Wilson, 1986). It is attractive, because of the similarity between psychophysically determined filter properties and the physiological properties of single neurons in macaque striate cortex (De Valois, Albrecht, & Thorell, 1982; De Valois, Yund, & Hepler, 1982; Hubel & Wiesel, 1968; Parker & Hawken, 1985).

Improvement in Vernier acuity due to intensive training suggests that the functional properties of offset analysing mechanisms are not hardwired and fixed, but highly adaptive. Saarinen and Levi (1995) examined, whether improvement in Vernier acuity due to training is accompanied by changes of the orientation tuning characteristics as revealed by a simultaneous spatial masking paradigm. The authors revealed a close correspondence between improvement in Vernier acuity and a specific narrowing and downward translation of the orientation tuning curve. Their results implied that neural plasticity located early in the visual pathway is a possible key mechanism of perceptual learning of

* Present address: Ruhr-Universität, AE Biopsychologie, GAFO 05/621 Universitätsstr. 150, D-44780 Bochum, Germany. Tel.: +49-234-32-24032; fax: +49-234-32-14377.

E-mail address: kristian.folta@ruhr-uni-bochum.de (K. Folta).

0042-6989/03/$ - see front matter
doi:10.1016/S0042-6989(03)00041-5

Vernier acuity (Kirkwood, Rioult, & Bear, 1996; Saarinen & Levi, 1995).

The present study further investigates the mechanisms allowing for increased acuity with training in Vernier discriminations. Before and after intensive training in an unmasked Vernier discrimination task orientation tuning of offset analysing mechanisms had been measured using a masking technique, similar to the technique applied by Saarinen and Levi (1995). The novelty of the present study lies in the additional use of subthreshold summation techniques (Kulikowski & King-Smith, 1973; Watson, 1982) to compare summation index functions in pre- and post-tests. Those functions reflect orientation tuning of offset analysing mechanisms, too, and probe the effect of Vernier training on orientation detectors in a sensible way.

In the case of neural fine tuning specific changes of orientation tuning had been expected, i.e. a narrowing of masking tuning functions in the near of peak masking orientation and a narrowing of summation index functions for superimposed Gabor patches, if the first orientation component was oriented at peak masking orientation and the second component was varied.

The results of the present study confirm the existence of learning related changes at early levels of visual processing, but the data cannot be easily explained by fine tuning of orientation tuned mechanisms. Instead, explanations based on stimulus enhancement due to broadening of specific orientation tuned mechanisms will be discussed.

2. General methods

2.1. Apparatus and stimuli

All patterns were generated using a VSG2/3 stimulus generator and were displayed on an EIZO FlexScan 6600M 21″ grayscale monitor. The refresh rate of the monitor was 82 Hz with a horizontal frequency of 67.8 kHz. The resolution was set to 1024×768 pixels. The mean luminance of the screen was set to 50 cd/m^2. The room was darkened such that the ambient illumination matched the illumination on the screen to a fair degree of approximation. Patterns were viewed monocular at a distance of 450 cm, with ambient luminance provided by the monitor. The subjects used a chin rest and an ocular, which limited the visible area of the screen to a circular field of 216′ in diameter. Subjects signaled their decisions on an external response box.

2.1.1. Gabor masks

Gabor masks consisted of oblique sinusoidal gratings, each 60′ in width and 60′ in length, spatially bounded by a smooth radial symmetric Gaussian envelope. The contrast of all Gabor masks was fixed at 30%. Mask spatial frequency was always 8 cpd and all masks could be randomly oriented either 0°, 8°, 16°, 20°, 24°, 32° or 60° clockwise from vertical. Mask phase was randomized in each trial of each experimental session. Fig. 1 shows examples of Gabor masks as they are used in this study.

2.1.2. Vernier stimuli

Vernier line stimuli consisted of two short abutting vertical dark line segments, each 0.54′ in width and 30′ in length presented on a mean luminance background. All stimuli were shown with suprathreshold Maxwell contrast of $m_c = 0.18$, which was far above detection threshold. In all threshold measurements the lower segment of the Vernier stimulus was displaced at one of five possible offsets, representing four equal horizontal offsets to the right of alignment, including a no- offset condition. The step size of these offsets was chosen on the basis of pilot experiments, to be close to the observers threshold and appropriate for all stimulus and mask conditions used. Simultaneous presentation of oblique Gabor mask patterns and Vernier line segments was accomplished simply by local superposition of mask and Vernier stimulus (see example in the lower right of Fig. 1). Figural representations of Vernier/mask configurations were provided at the beginning of the experiment.

2.1.3. Compound Gabor stimuli

Detection thresholds were measured concurrently for three sinusoidal stimuli: a patch of orientation θ_1, a patch of orientation θ_2, and a patch containing both orientations θ_1 and θ_2. Spatial frequency was always 8 cpd. Examples of compound Gabor stimuli are shown in Fig. 2.

In each stimulus, the luminance at a point x, y was specified by

$$L(x,y) = L_0[1 + w(x,y)m(x)] \tag{1}$$

where L_0 defines the mean luminance of the screen (which was set to 50 cd/m^2). The term $m(x)$ is the sum of two sinusoidal components of orientations θ_1 and θ_2 and (pre-windowed) contrasts c_1 and c_2,

$$\begin{aligned} m(x) = {} & c_1 \sin[2\pi f(x\cos(\theta_1(\pi/180)) \\ & + y\sin(\theta_1(\pi/180)))] \\ & + c_2 \sin[2\pi f(x\cos(\theta_2(\pi/180)) + y\sin(\theta_2(\pi/180)))] \end{aligned} \tag{2}$$

All patches were spatially bounded by a smooth radial symmetric Gaussian envelope,

$$w(x,y) = \exp[-0.5((x^2 + y^2)/s_{x,y}^2)] \tag{3}$$

where $s_{x,y}$ denotes the spread of the Gaussian. Horizontal and vertical spreads were always equal, and were set to 1.5°.

Simultaneous presentation of both components was accomplished simply by local superposition. For com-

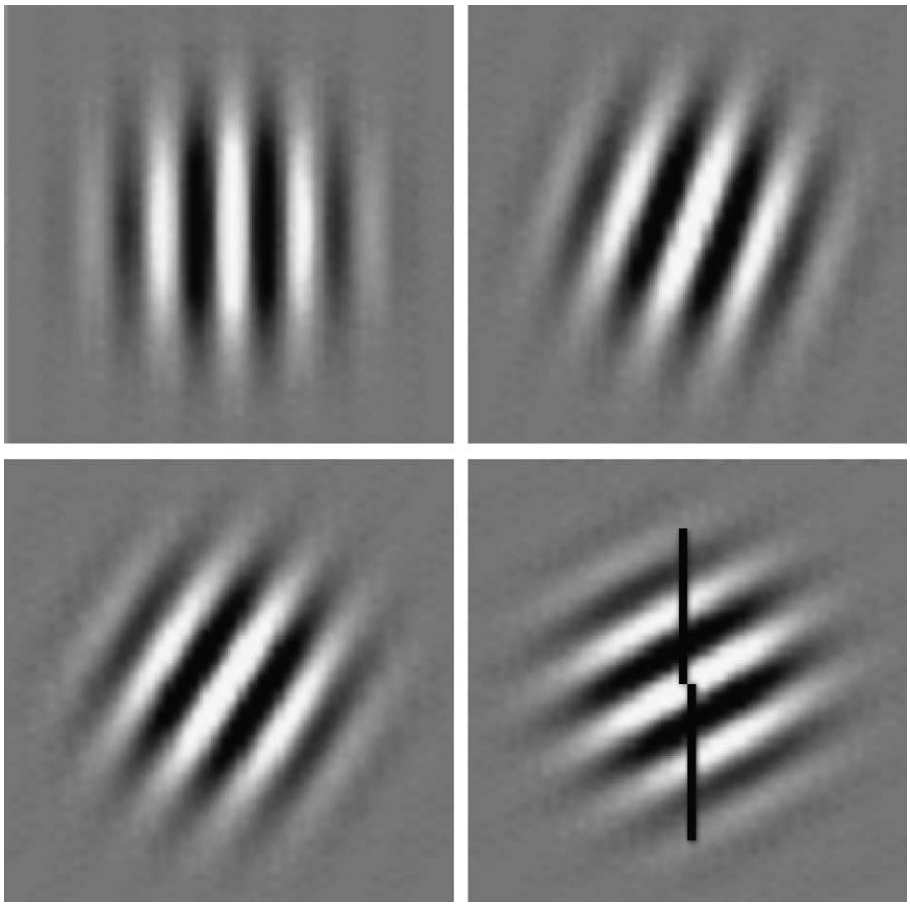

Fig. 1. Gabor masks oriented 0° (upper left), 20° (upper right), 32° (lower left) and 60° clockwise from vertical (lower right). The example in the lower right shows a superposition of mask and Vernier stimulus.

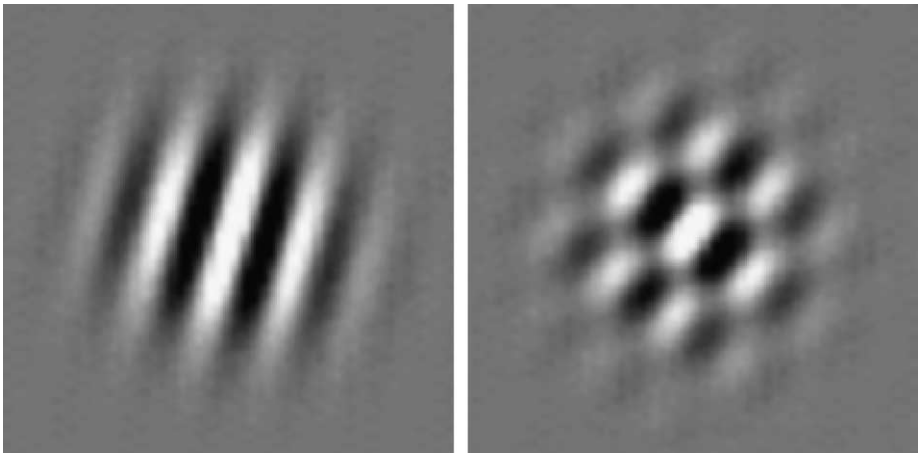

Fig. 2. Examples of compound Gabor stimuli. The orientation of the first component is always $\theta_1 = 12°$. The second component is $\theta_2 = 20°$ (left) and $\theta_2 = 60°$ (right).

pound gratings the orientation of the first patch was always $\theta_1 = 12°$, the second component θ_2 was either 16°, 20°, 24°, 32° or 60° clockwise from vertical. The orientation of the first patch ($\theta_1 = 12°$) was chosen on the basis of subjects masking data and represents the mean peak masking orientation of masking tuning functions measured for each subject.

2.2. Discrimination thresholds for masked and unmasked Vernier stimuli

Vernier thresholds for discriminating an unidirectional Vernier offset were measured using a yes–no discrimination task: A ready tone was accompanied by a 500 ms blanc screen. After that time interval subjects

were exposed to one of eight randomly selected Vernier stimuli. These stimuli could be either one of four targets with offsets to the right, or one of four identical distractors with no offset. Stimulus duration was 750 ms. Pattern presentation was done using temporally fading in and out according to a trapezian function (125 ms rise and fade time of a linear ramp, 500 ms plateau time). The observer's task was to judge whether the presented stimulus has an offset to the right or not. Trial by trial acoustical feedback was provided about correctness for each yes/no judgement which the subjects made via an external response keyboard with two buttons (yes/no). Each distractor and target was presented with equal probability (25 times in a block of 200 trials, i.e. one session comprised of 200 trials).

Based on the offset, metrical discrimination thresholds were calculated according to the signal detection paradigm. For each of the four targets hit and false alarm rates were calculated and z-transformed. The mean of four correct rejections of each distractor was calculated, z-transformed and used for estimation of individual d' values. These four d' values were inserted in a diagram (Fig. 3) showing the offset sizes on the abscissa and d' values on the ordinate. A regression line was calculated and the linearity was checked for each threshold measurement. In most of the cases the determination coefficient of the linear regression was larger than 0.8. From this linear regression the offset Δx_0 corresponding to $d' = 1.5$ was calculated and used as an estimation of the discrimination threshold (see Fig. 3). This threshold represents the smallest offset size which the observer could discriminate at $d' = 1.5$ from no offset.

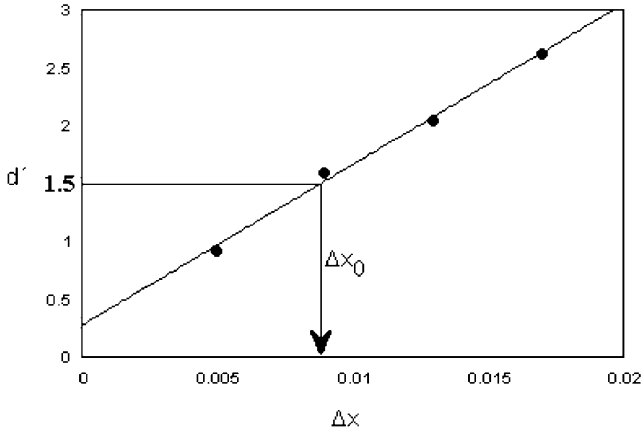

Fig. 3. Illustration of d' scaling used in order to estimate metrical discrimination thresholds. Data are shown for a session of a typical Vernier discrimination task. For each offset the corresponding d' values were calculated from the hit and false alarm rates. A linear regression was applied, which generally yielded a very good fit for the data of the experiment. A value of $d' = 1.5$ was used as threshold criterion. The arrow marks the extrapolated discrimination threshold Δx_0 obtained from this criterion for one block of trials.

Threshold estimations for masked Vernier stimuli in pre- and post-test comprised of four sessions for each mask-orientation measured on four consecutive days.

During discrimination training in the absence of any mask one training day comprised of three sessions with 200 trials.

2.3. Detection thresholds for compound Gabor stimuli

Detection thresholds for compound Gabor stimuli were measured in order to determine orientation tuning by means of summation index functions. These functions, reflecting the degree of joint activation of the detecting analysers, were used to evaluate sensory changes of offset analysing mechanisms due to Vernier acuity training.

Four experimental sessions were carried out at four consecutive days with each subject. Within each experimental session the contrast threshold for five compound patches (θ_1 = peak masking orientation, $\theta_2 = 16°$, 20°, 24°, 32° or 60°) and six possible simple grating patches (12°, 16°, 20°, 24°, 32° and 60°) were determined. The contrast of the second component c_2 was chosen in a way that both orientation components had approximately the same relative component strength at threshold. In order to determine the appropriate value of c_2, measurements of thresholds for simple gratings were carried out prior to measurement of compound grating thresholds.

Within each experimental session the threshold contrast for each of the five compounds and six simple patterns was measured five times according to a random list, i.e. one session comprised of 55 trials. Contrast thresholds were measured using the method of limits. The contrast c_1 was fixed at threshold and the contrast of the second component c_2 was varied. The results of five threshold measurements for compound patches were plotted in contrast interrelation diagrams (Fig. 4). Let c_1^* and c_2^* be the average contrast thresholds for the θ_1- and θ_2-components alone. The abscissa specifies the contrast of the θ_1-component of the compound, divided by the average threshold contrast for the θ_1-component alone, or c_1/c_1^*. The ordinate indicates the contrast of the θ_2-component of the compound, divided by the average threshold for that component alone, or c_2/c_2^*. The thresholds for compound patches lie in the upper right of the graph. Since the contrast ratio of the two components was re-adjusted before each session, the points do not lie on a common ray from the origin. However, a single measurement of summation can be derived (Watson, 1982). Let c_1 and c_2 be the contrasts of the two components in a compound patch. A parameter M ($\geqslant 0$) defines a unique contour of the form

$$1 = (c_1/c_1^*)^M + (c_2/c_2^*)^M \tag{4}$$

which intersects the three points $(c_1^*, 0)$, $(0, c_2^*)$, and (c_1, c_2). The contour for two compounds are sketched in

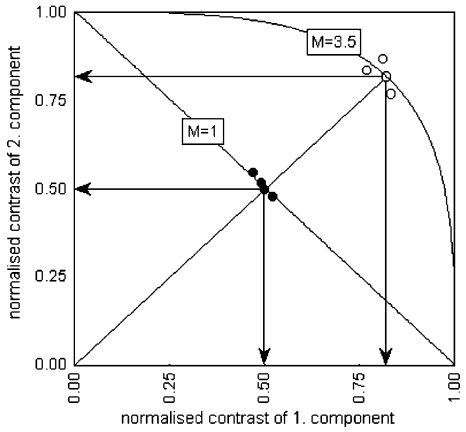

Fig. 4. Contrast interrelation measurements for compound Gabor gratings in the normalised contrast space (hypothetical data) for close ($M = 1$, solid circles) and far apart values ($M = 3.5$, open circles) of orientation separation $\Delta\theta$. The intersection of the smooth contour with the ray is a good estimate of the contrast that would have been obtained if the measurement had been along the ray (Watson, 1982).

Fig. 4. This figure shows examples of compounds given values of $M = 1$ and $M = 3.5$. Of special interest were measurements that lay exactly on the 45° ray, since they could be used as a measurement of component summation. While it was difficult to obtain measurements lying exactly on the 45° ray, the intersection of the smooth contour (4) with the ray was a good estimate of the contrast that would have been obtained if the measurement had been along the ray (Watson, 1982). At this point we obtained the summation index SI for compound patterns at threshold,

$$\mathrm{SI} = 2^{1/M} \tag{5}$$

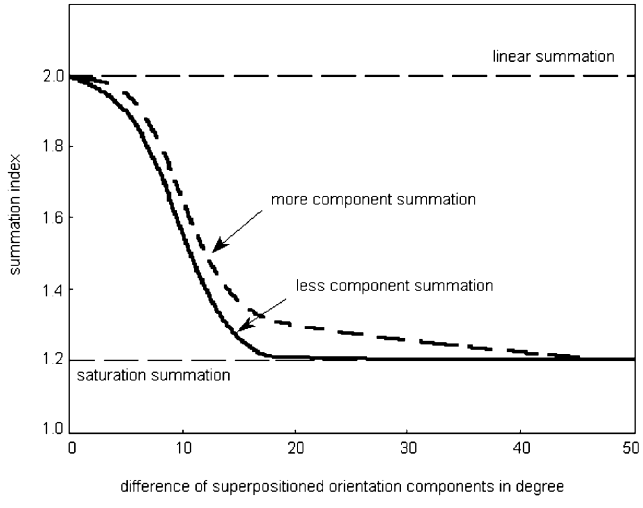

Fig. 5. Illustration of the summation index, obtained from normalised contrast interrelation data (see Fig. 4). Two hypothetical summation index curves are shown. If there is low component summation, a more narrow summation index curve results. A large amount of component summation causes the summation index function to broaden.

The summation index, as obtained from contrast interrelation data, reflects orientation component summation, following a smooth non-linear tuning curve as indicated by the two (hypothetical) solid lines in Fig. 5. If there is low component summation, a more narrow summation index curve results, a large amount of component summation causes the function to broaden. Summation declines rapidly with increasing separation between the component orientations, so that an octave away only an amount consistent with probability summation remains. The summation index (5) is therefore a comfortable measurement of the joint activation of offset analysing mechanisms.

3. Experiment

3.1. Methods

3.1.1. Observers

Three observers participated in this study. With the exception of NK the subjects were male. No pre-testing was employed for selecting the observers. All observers had normal or corrected-to-normal vision. NK was a novice in psychophysical tasks, all other subjects were well experienced observers, but none of them had any prior experience in Vernier acuity tasks. Subjects were paid for participation and were well motivated but naive with regard to the purpose of the study.

3.1.2. Stimuli and procedures

All stimuli and general procedures are described in Section 2. This study was designed as a pre-test-discrimination learning-post-test measurement. During training, three sessions of 200 trials were carried out per day. All subjects learned on 10 consecutive days (interrupted by a weekend break of two days), until the moving averages of the unmasked Vernier threshold data indicated that saturation was reached to a fair degree. All observers were informed about their progress as the training proceeded. Before and after training Vernier discrimination thresholds (according to a masking paradigm) and detection thresholds (according to a summation to threshold paradigm) were determined.

Table 1
Summary of the pre-test-training-post-test-rationale

Pre-test/post-test	Training
A Masking tuning functions (four sessions for each mask orientation/ 200 trials per session) B Detection tuning functions (four sessions at consecutive days/55 trials per session)	Vernier-discrimination without masking (three sessions per day/200 trials per session)

After 10 days of training in unmasked Vernier acuity post-test measurements were done, arranged in exactly the same manner as in the pre-test. Before each post-test measurement subjects did three unmasked Vernier discrimination sessions of 200 trials per day in order to control for stability of learning. Table 1 gives a summary of the pre-test-training-post-test-rationale used in this study.

4. Results

4.1. Unmasked Vernier thresholds during acuity training

Fig. 6 shows the course of intensive unmasked Vernier discrimination training for each of the three observers. All subjects learned and show substantial reduction of their Vernier discrimination thresholds during the course of training. As it is standard in perceptual learning, the fastest changes are observed early in training. The mean discrimination threshold across subjects was 1.176′ in the first three and 0.63′ in the last three sessions, i.e. a decrease in Vernier threshold from 46%, which is a remarkable resolution for blurred objects presented in a distance of 450 cm. For that reason, all subjects can be considered as highly trained after ten days of learning.

To judge statistical significance of the improvement, learning data were subjected to an ANOVA. Most important, the F-ratio for the training day factor reaches 5% significance level for all subjects (TH: $F(16,32) = 2.70$, $p < 0.008$; NK: $F(16,32) = 2.42$, $p < 0.016$; FA: $F(16,32) = 4.83$, $p < 0.00008$). All subjects reached their individual saturation limit of performance to a fair degree at the 11th day of training, when orientation tuning post-tests began. The differences of the slope of individual learning curves were striking and in agreement with previous learning studies (Fahle & Edelman, 1993; McKee & Westheimer, 1978). For instance, McKee and Westheimer (1978) reported that after 2000–2500 practice trials, the range of the individual decrease in Vernier thresholds was from 2% to 70%. This individual variation might have been even larger if they had not employed a pre-test for selecting their observers. In their pre-test, those individuals were screened to serve as observers, who had the best initial Vernier thresholds.

4.2. Masked Vernier thresholds

Since one of the main interests of this study was to assess the effect of training on the shape of individual tuning functions, initially obtained masked Vernier thresholds had been compared to those, obtained at the end of the training. Individual Vernier thresholds before (solid circles) and after practice (solid squares) are shown in Fig. 7.

It was of particular interest, whether there was a narrowing of the orientation tuning after training. The present results reveal no narrowing of the orientation tuning characteristics, i.e. there was a general improvement of masked Vernier thresholds for all mask orientations. Before and after practice the peak masking orientation of the three observers was between 10° and 20°. This result is in line with previous reported data from studies of orientation masking of Vernier acuity, showing peak threshold elevations at about 10°–20° on each side of Vernier target orientation (Carney & Klein, 1991; Findlay, 1973; Levi & Waugh, 1996; Mussap & Levi, 1995, 1996, 1997; Saarinen & Levi, 1995; Waugh et al., 1993).

In the present study, the masking functions of all three subjects are standard up to 24° of mask orientation, but then the thresholds rise again, showing a dip in the region of 24°. This effect is not in line with previous reported data and might be a consequence of stimulus interferences produced by simple superposition of mask and Vernier stimulus.

To judge statistical significance of threshold improvement and peak masking effect the tuning data were analysed with an ANOVA with the factors subject (grouping), time of measurement (repeated measure-

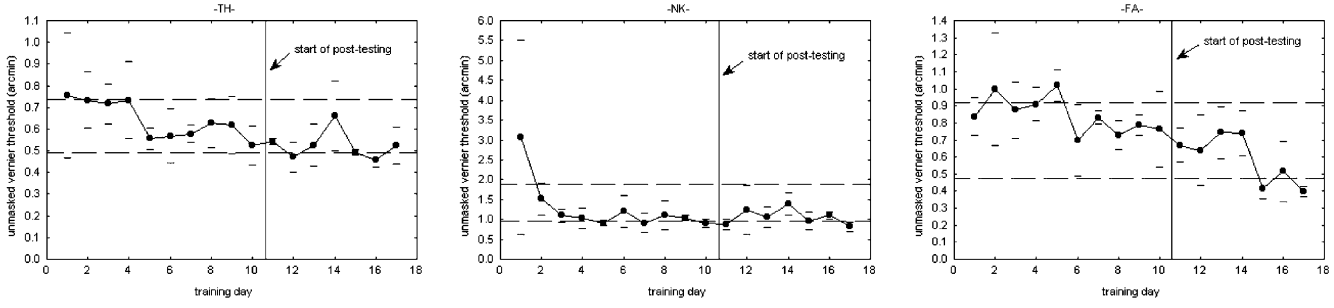

Fig. 6. Unmasked Vernier discrimination thresholds as a function of training day, as extrapolated from a fixed discrimination criterion of $d' = 1.5$. Each solid circle represents the average of three training sessions per day and the error bars mark the 95% confidence interval for each day. The averages of the first three and last three learning days are shown as horizontal dashed lines. Arrows mark the begin of post-testing.

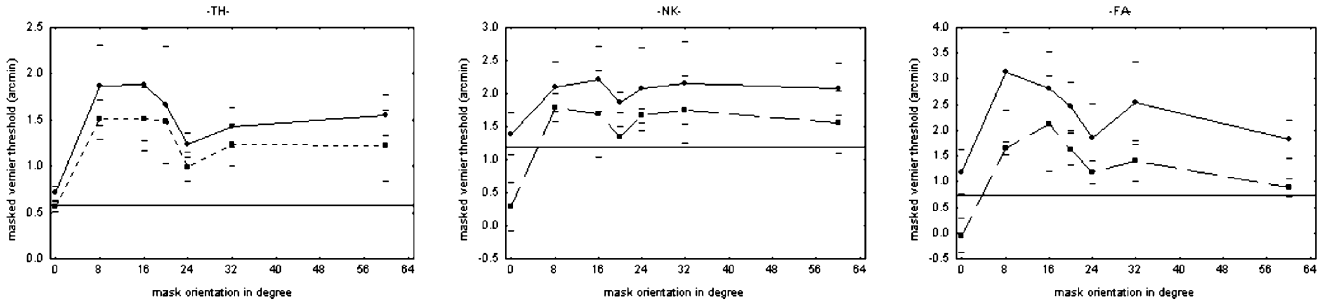

Fig. 7. Masked Vernier thresholds plotted against mask orientation before (solid circles) and after training (solid squares). Thresholds are extrapolated from a fixed discrimination criterion of $d' = 1.5$. Error bars mark the 95% confidence interval. Unmasked Vernier thresholds are indicated by horizontal lines.

ment) and mask orientation (repeated measurement). Most important, the F-ratio for the time ($F(1,9) = 44.74$, $p < 0.00009$) and orientation factor ($F(6,54) = 33.4$, $p < 0.00001$) reaches 1% significance level. The effect of measurement time on orientation tuning functions does not depend on the subject or any mask orientation. This also becomes apparent at the between subject averaged tuning data, as illustrated in Fig. 8. The post-test function is an almost constant shifted version of the curve observed in the pre-test.

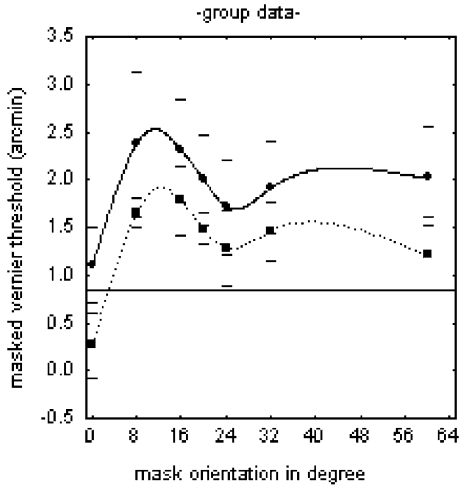

Fig. 8. Between subject averaged tuning data of masked Vernier thresholds before (solid circles) and after training (solid squares). Thresholds are extrapolated from a fixed discrimination criterion of $d' = 1.5$. Error bars mark the 95% confidence interval of each threshold measurement. The unmasked Vernier threshold is indicated by a horizontal line.

To summarize, because thresholds generally decrease after training and decrease not relatively more at those mask orientations which were away from the orientations producing the peak threshold elevation, explanations based on fine tuning of individual orientation tuned analysers may be excluded.

4.3. Detection tuning functions

To further exclude that no fine tuning of offset analysing mechanisms takes place during the course of training a summation to threshold paradigm in pre- and post-tests was additionally used to measure sensory changes of offset-analysing mechanisms. Fig. 9 shows summation index functions obtained in pre- and post-tests. The summation index curves monotonously decline with increasing difference of orientation components of a compound patch. Regarding the within subject comparison of pre-test and post-test measurements a broadening effect due to training was observed. In the post-test (solid squares) all subjects show larger values of component summation than in the pre-test (solid circles). Orientation differences of $\Delta\theta = 0°$ have per definition always values of 2, because detection of

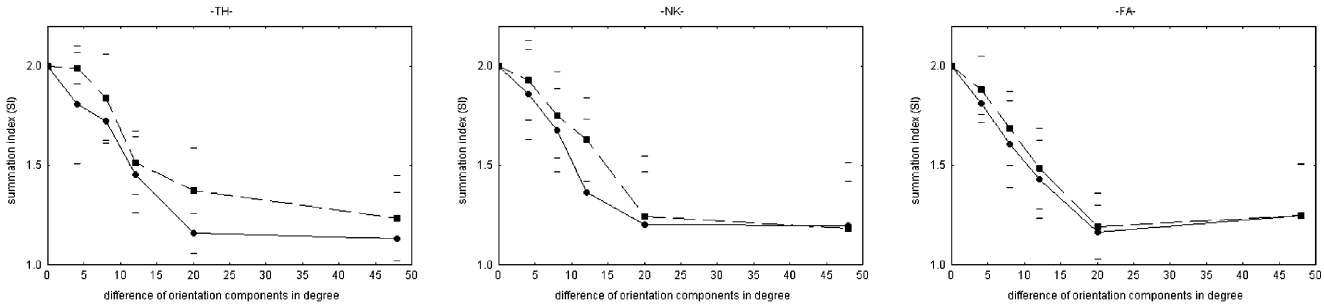

Fig. 9. Summation index functions before (solid circles) and after training (solid squares). Data are shown for all subjects. Error bars mark the 95% confidence interval for each measurement.

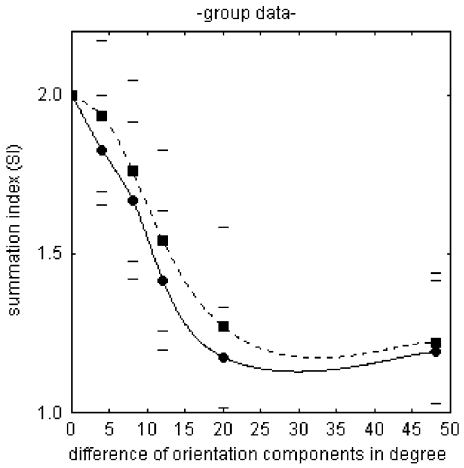

Fig. 10. Between subject averaged summation index data before (solid circles) and after training (solid squares). Error bars mark the 95% confidence interval for each measurement.

compound patches of identical components is the same as detection of one component alone. Secondly, it is expected that compound patches, consisting of components with large orientation differences ($\Delta\theta = 50°$), activate independent mechanisms. At $\Delta\theta = 50°$ there is no analyser which is sensitive to both orientation components and no summation other than the remaining nonlinear pooling gain is present.

To judge statistical significance of larger values of component summation the data were analysed using an ANOVA with the factors subject (grouping), time of measurement (repeated measurement) and orientation difference of the orientation components of a complex Gabor patch (repeated measurement).

Most important, the F-ratio for the time ($F(1,9) = 428.27$, $p < 0.00001$) and orientation factor ($F(4,36) = 321.65$, $p < 0.00001$) reaches 1% significance level. The effect of measurement time on detection tuning functions does not depend on the subject or specific orientation differences. This becomes apparent at the between subject averaged tuning data, as illustrated in Fig. 10.

The result that observers became more sensitive to orientation combinations in the near of peak masking orientation during Vernier acuity training is compatible with the notion of neural changes in orientation tuning of mechanisms sensitive to peak masking orientation. In this study those mechanisms become broader tuned during Vernier acuity training, which are believed to be most important for detecting Vernier offsets.

5. General discussion

In the present study a masking and subthreshold summation paradigm was employed to further explore the role of neural plasticity and fine tuning of offset analysing mechanisms during unmasked Vernier acuity training.

The present results confirm the existence of learning related changes at early levels of information processing, but the results cannot be easily explained by neural fine tuning of offset analysing mechanisms.

In the case of fine tuning a selective narrowing of orientation masking tuning curves in the near of peak masking orientation was expected. But the present results reveal a general reduction of Vernier thresholds after training, irrespectable of mask orientation. These results seem to contradict to the second finding of the present study that all subjects show broadening of their summation index functions after training. Broader summation index functions reveal more joint activation of mechanisms responsible for signalling Vernier offsets (i.e. mechanisms that are tuned to peak masking orientation) and mechanisms tuned to orientations in the near of peak masking orientation. By broadening the response tuning of offset analysing mechanisms larger neural outputs are elicited for orientation cues in the near of peak masking. This increases the stimulus strength or encoding efficiency of non-aligned Vernier lines. After training, offset analysing mechanisms (tuned to $\pm 12°$ orientations) become strongly activated, not only in the presence of 12° orientation cues, but also in the presence of orientation cues in the near of peak masking orientation. Since the only task of subjects during training was to decide about vertical orientation (alignment) or non-vertical orientation (non-alignment of Vernier lines) broader tunings might be better for the detection of small offsets from vertical (i.e. orientations in the near of peak masking orientation). As a consequence, observers show higher hit rates and correct rejection rates after training, i.e. a general reduction of masked Vernier thresholds irrespective of mask orientation.

Although this study is strongly rooted in the previous work by Saarinen and Levi (1995), small experimental changes in the present study lead to different results in the measurement of orientation masking tuning functions.

The main difference of the present study and the work by Saarinen and Levi (1995) lies in the kind of Vernier task observers had to fulfil. In the present study observers had to judge whether the presented stimulus had an offset to the right or not. Subjects made their yes/no judgements by pressing a yes- or a no-button. Saarinen and Levi's (1995) observers rated not only the presence or absence of an offset, but rated the offset size (0, 1, 2, or 3) and gave their responses by pressing one of four keys in the response box.

Different neural mechanisms might be involved in both tasks. A narrowing of orientation tuning might be a good and efficient neural strategy in the case of identification of different offset sizes. In the case of simple

yes/no-discriminations a more effective strategy might be to broaden the orientation tuning of mechanisms, which are responsible for detecting small offsets (i.e. orientations in the near of peak masking). In both cases a downward translation of the orientation masking tuning curve is expected after training. Further experiments are necessary to clarify the role of task dependent changes of orientation tuning in Vernier acuity.

Acknowledgements

I am grateful to Günter Meinhardt and Uwe Mortensen for their generous help and excellent technical support and to Daniela Schoofs, Bettina Diekamp, Onur Güntürkün and an anonymous reviewer for helpful comments to the manuscript.

References

Carney, T., & Klein, S. A. (1991). Orientation masking of grating Vernier acuity. *Investigative Ophthalmology and Visual Science, 32*(Suppl.), 1023.

De Valois, R. L., Albrecht, D. G., & Thorell, L. G. (1982). Spatial frequency selectivity of cells in the macaque visual cortex. *Vision Research, 22*, 545–559.

De Valois, R. L., Yund, E. W., & Hepler, N. (1982). The orientation and direction selectivity of cells in macaque visual cortex. *Vision Research, 22*, 531–544.

Fahle, M., & Edelman, S. (1993). Long term learning in Vernier acuity: effects of stimulus orientation, range and of feedback. *Vision Research, 33*, 397–412.

Findlay, J. M. (1973). Feature detectors and Vernier acuity. *Nature, 241*, 135–137.

Hubel, D. H., & Wiesel, T. N. (1968). Receptive fields and functional architecture of monkey striate cortex. *Journal of Physiology, 195*, 225–243.

Kirkwood, A., Rioult, M. G., & Bear, M. F. (1996). Experience dependent modification of synaptic plasticity in visual cortex. *Nature, 381*, 526–528.

Kulikowski, J. J., & King-Smith, P. E. (1973). Spatial arrangement of line, edge and grating detectors revealed by subthreshold summation. *Vision Research, 13*, 1455–1478.

Levi, D. M., & Waugh, S. J. (1996). Position acuity with opposite polarity features: evidence for a nonlinear collator mechanism for position acuity? *Vision Research, 36*, 573–588.

McKee, S. P., & Westheimer, G. (1978). Improvement in Vernier acuity with practice. *Perception & Psychophysics, 24*, 258–262.

Mussap, A. J., & Levi, D. M. (1995). Binocular processes in Vernier acuity. *Journal of the Optical Society of America A, 12*, 225–233.

Mussap, A. J., & Levi, D. M. (1996). Spatial properties of filters underlying Vernier acuity revealed by masking: evidence for collator mechanisms. *Vision Research, 36*, 2459–2473.

Mussap, A. J., & Levi, D. M. (1997). Vernier acuity with plaid masks: the role of oriented filters in Vernier acuity. *Vision Research, 37*, 1325–1340.

Parker, A., & Hawken, M. (1985). Capabilities of monkey cortical cells in spatial resolution tasks. *Journal of the Optical Society of America, 2*, 1101–1114.

Saarinen, J., & Levi, D. M. (1995). Perceptual learning in Vernier acuity: what is learnt? *Vision Research, 35*, 519–527.

Watson, A. B. (1982). Summation of grating patches indicates many types of detector at one retinal location. *Vision Research, 22*, 17–25.

Waugh, S. J., Levi, D. M., & Carney, T. (1993). Orientation, masking and Vernier acuity for line targets. *Vision Research, 33*, 1619–1638.

Westheimer, G. (1975). Visual acuity and hyperacuity. *Investigative Ophthalmology and Visual Science, 14*, 570–572.

Wilson, H. R., & Gelb, D. J. (1984). Modified line-element theory for spatial-frequency and width discrimination. *Journal of the Optical Society of America A, 9*, 124–131.

Wilson, H. R. (1986). Responses of spatial mechanisms can explain Vernier acuity. *Vision Research, 26*, 453–469.